Dental Materials Journal 2019; 38(5): 798–805

The effect of flowable composite lining and dentin location on microtensile bond strength and internal fracture formation

Nao KOMINAMI[1], Yasushi SHIMADA[2], Keiichi HOSAKA[1], Minh Nguyet LUONG[3,4], Masahiro YOSHIYAMA[2], Alireza SADR[4], Yasunori SUMI[5] and Junji TAGAMI[1]

[1] *Department of Cariology and Operative Dentistry, Graduate School of Medical and Dental Sciences, Tokyo Medical and Dental University, 1-5-45, Yushima, Bunkyo-ku, Tokyo 113-8549, Japan*

[2] *Department of Operative Dentistry, Graduate School of Medicine, Dentistry and Pharmaceutical Sciences, Okayama University, 2-5-1, Shikata-cho, Kita-ku, Okayama 700-8525, Japan*

[3] *Department of Restorative Dentistry and Endodontics, Faculty of Odonto-Stomatology, University of Medicine and Pharmacy at Ho Chi Minh City, 652, Nguyen Trai, District 5, Ho Chi Minh City, Vietnam*

[4] *Biomimetics Biomaterials Biophotonics & Technology Laboratory, Department of Restorative Dentistry, University of Washington School of Dentistry, 1959 NE Pacific St. Box 357456, Seattle, WA 98195-7456, USA*

[5] *National Center for Geriatrics and Gerontology, Department of Advanced Dental Research, Center of Advanced Medicine for Dental and Oral Disease, 7-430, Morioka, Obu, Aichi 474-8511, Japan*

Corresponding author, Yasushi SHIMADA; E-mail: shimada.ope@okayama-u.ac.jp

The objective of this study was to determine the effect of flowable composite lining and dentin location on internal dentin fracture formation in the microtensile bond strength (MTBS) test using swept-source optical coherence tomography (SS-OCT). MTBS test beams (1.0×1.0 mm) were prepared from human superficial and deep dentin, which was bonded with a self-etch adhesive (Clearfil SE Bond) and hybrid composite resin (Clearfil AP-X), with or without flowable lining (Clearfil Majesty ES-Flow). We tested 4 groups according to placement technique (with *vs.* without flowable liner) and dentin (superficial *vs.* deep) locations. Cross-sectional 2D images of the bonded interface were obtained before and after the MTBS test. Internal dentin fracture after MTBT was observed as a bright zone in SS-OCT. Flowable lining significantly reduced internal fracture formation in dentin ($p<0.05$). Dentin location significantly influenced MTBS ($p<0.05$), and this was reduced by flowable lining usage.

Keywords: Dentin, Internal fracture, SS-OCT, Microtensile bond strength test

INTRODUCTION

Resin composite material became the first choice for direct dental restoration due to its excellent esthetic appearance and minimally invasive therapy. Despite widespread utilization of resin composite to recover the function and esthetics of teeth, composite materials suffer contraction stress during polymerization that can cause an interfacial gap[1]. Consequently, it remains challenge to achieve a perfect marginal seal in restorations. The use of the adhesive system with low-viscosity resin can improve bond strength and interfacial adaptation of restorative composites to dentin[1-9]. Low-viscosity resin with a low elastic modulus can act as a stress-absorbing layer to preserve the integrity of structures[2,9]. The application of low-viscosity resin has possibility to decrease the crack formation in dentin through absorbing energy and protecting the substrate[10]. Moreover, several lines of evidence have shown that two step self-etch adhesives containing MDP monomer can produce excellent bonds and high durability to dentin[11-13]. Therefore, a lining technique using a flowable composite at the cavity floor combined with self-etch adhesives is recommended to achieve well performance of tooth restoration[4,5,10].

The microtensile bond strength (MTBS) test has widely been used to screen the bonding performance of adhesive systems because it can evaluate the bond strength of a small area in the complexity of bonded substrate[14,15]. Previous studies have revealed that the bond strength of dentin adhesives is dependent on the microstructure of the dentin substrate, which altered with depth[16,17].

At different dentin depth, the percentage tubular area and diameter vary from approximately 22% and 2.5 μm, respectively, near the pulp to 1% and 0.8 μm, respectively, at the dentinoenamel junction (DEJ)[18]. Another study has shown that the microhardness of dentin decreases from the DEJ towards the pulp with a corresponding increase in tubule density[19]. These structural differences influence the bond mechanism and strength of resin to dentin.

Optical coherence tomography (OCT) is a new imaging device that uses the interferometric technique. OCT creates cross-sectional images by measuring the backscattered signal intensity from inside of a structure. Its applications in dentistry include assessing dental caries[20-22], monitoring defects of restoration[8,23,24], and determining tooth crack locations[10,25,26]. Recently, the influence of crosshead speed in the MTBS test, and placement technique in bond strength and dentin crack formation after MTBS test has been assessed using swept-source OCT (SS-OCT)[10]. However, the influence of dentin depth on structural damage after MTBS test has not been fully elucidated, in part due to limited conventional *in vitro* microscopic imaging methods.

The aim of this study was to determine the influence of dentin depth on bonding, with and without flowable

Received Jul 18, 2018: Accepted Dec 3, 2018
doi:10.4012/dmj.2018-232 JOI JST.JSTAGE/dmj/2018-232

composite lining using SS-OCT. The null hypothesis was that: there was no influence of dentin location and placement technique on MTBS and internal dentin fracture formation after the MTBS test.

MATERIALS AND METHODS

OCT system

The SS-OCT (IVS-2000, Santec, Komaki, Japan) is a frequency domain OCT technique that measures the magnitude and time delay of reflected light in order to construct a depth profile[21]. The SS-OCT system used in this study incorporated a high-speed frequency swept external cavity laser with a probe power is less than 5 mW within the American National Standards Institute limit, center wavelength of 1,319 nm, and scan rage of 112 nm at a 20 kHz sweep rate[21]. Briefly, the focused light beam is projected onto selected locations and scanned across the area of interest in two dimensions (X, Y) using a hand-held probe. Backscattered light from the sample is coupled back to the system, onto a digitized in time scale, and analyzed in the Fourier domain to reveal depth information of the subject (A-scan). The resulting series of A-scans along the area of interest are combined to generate two dimensional cross sectional B-scan image. The axial resolution of the system is 12 μm in air, which corresponds to 7 μm in oral hard tissue, with a refractive index of approximately 1.5[10]. A lateral resolution of 20 μm is determined by the objective lens at the probe. The sensitivity of this system is 106 dB, and the shot-noise limited sensitivity is 119 dB[10].

Specimen preparation

We collected 40 extracted sound human molars as approved by the Institutional Review Board of Tokyo Medical and Dental University, Human Research Ethics Committee, protocol no. D2013-022. The procedures for sample preparation and visualization under OCT are illustrated in Fig. 1. After cleaning with a dental scaler and removal of the root, the coronal enamel was removed parallel to the occlusal surface using a water-cooled slow speed diamond saw (Isomet, Buehler, Lake Bluff, IL, USA). Two locations of dentin were obtained from the superficial and deep location to use in this study (Fig. 1a). Flat dentin surfaces with a standardized smear layer were prepared using wet-polished with 600-grit silicon carbide (SiC) paper (Sankyo, Saitama, Japan). The materials used in this study are listed in Table 1. The adhesive system was applied to the dentin surface according to the manufacturer's directions. The self-etching primer agent of Clearfil SE Bond (Kuraray Noritake Dental, Tokyo, Japan) was applied to the dentin surface for 20 s and gently blew by air. The SE Bond adhesive was cured using a halogen light curing unit (Optilux 501, Kerr, pCA, USA; 600 mW/cm^2 intensity) for 10 s. Two types of photo-cured composite

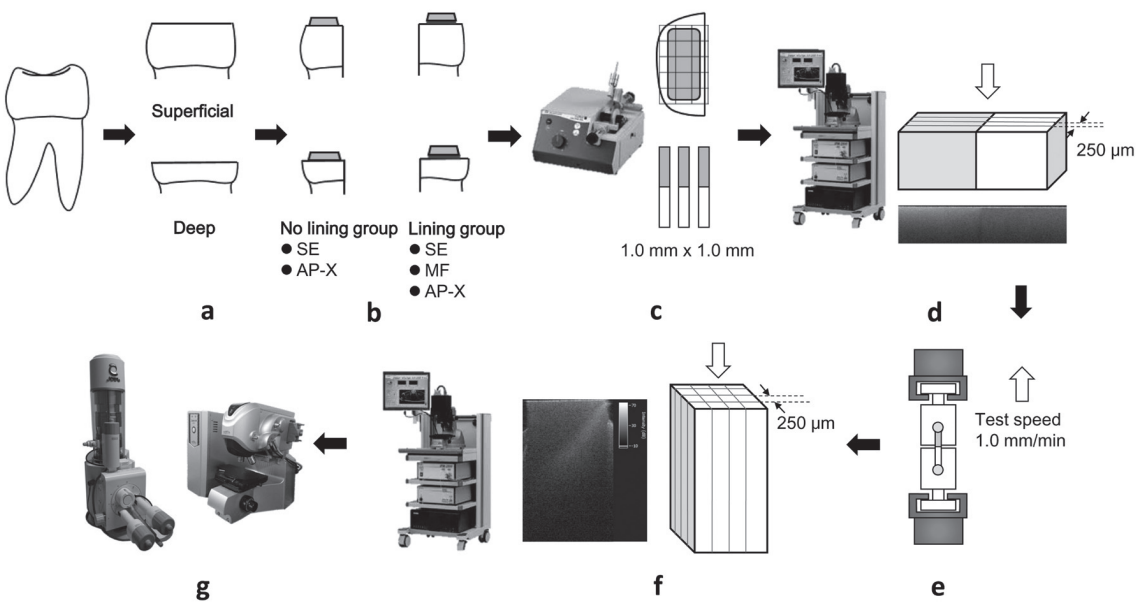

Fig. 1 Schematic view of sample preparation and visualization.
(a) The resin composite was applied in flat dentin with or without flowable composite lining and (b) beams were produced. (c) Two-dimensional cross-sectional images of the interface before the MTBS test were obtained with SS-OCT with the scanning beam perpendicular to the lateral side of the specimen. (d) The MTBS test was performed at a crosshead speed of 1 mm/min. (e) Debonded specimens were observed under SS-OCT after the test with the scanning beam perpendicular to the debonded interface. (f) Specimens were embedded and observed under confocal laser scanning microscopy and SEM to confirm the OCT findings. MTBS, microtensile bond strength; SS-OCT, swept-source optical coherence tomography; SE, Clearfil SE Bond; AP-X, Clearfil AP-X; MF, Clearfil Majesty ES-Flow.

Table 1 Materials used in this study

Material manufacturer	Composition			Lot no
Clearfil SE Bond (two-step self-etch adhesive) Kuraray Noritake Dental, Tokyo, Japan	Primer: MDP, HEMA, camphorquinone, hydrophilic dimethacrylate, N,N-diethanol p-toluidine, water. Bond: MDP, Bis-GMA, HEMA, camphorquinone, hydrophobic dimethacrylate, N,N-diethanol p-toluidine, silanated colloidal silica.			Primer: 9H0109 Bond: 9K0175
Material manufacturer	Resin matrix	Inorganic filler (Content)	Elastic modulus	Lot no
Clearfil AP-X (universal composite) Kuraray Noritake Dental	TEGDMA, Bis-GMA	silanated barium glass, silanated colloidal silica, silanated silica (85.0 wt%, 71.0 vol%)	18.4 GPa	340058
Clearfil Majesty ES-Flow (flowable composite) Kuraray Noritake Dental	TEGDMA, hydrophobic aromatic dimethacrylate	silanated barium glass, silanated silica (75.0 wt%, 59.0 vol%)	6.3 GPa	6A0232

MDP, 10-methacryloyloxyalkyl acid phosphate; HEMA, 2-hydroxyethyl methacrylate; TEGDMA, triethyleneglycol dimethacrylate; Bis-GMA, bisphenol-A-diglycidyl methacrylate

resin with different filler loading and elastic modulus was then built up on the surface (Table 1, data from manufacture information). A flowable composite resin, Clearfil Majesty ES Flow (Shade A2, Kuraray Noritake Dental) was applied as a lining on half samples from each dentin location, followed by an incremental addition of universal composite of Clearfil AP-X (Shade A2, Kuraray Noritake Dental). In the remaining samples, a single increment of universal resin composite was placed on the adhesive layer (Fig. 1b). Each composite resin was cured for 20 s with the light curing unit. After incubation in a water bath at 37°C for 24 h, the samples were sectioned into 1.0×1.0 mm beams perpendicular to the bonding interface using a water-cooled slow speed diamond saw (Fig. 1c). The beams were assessed prior to MTBS testing using SS-OCT to confirm the integrity of bonded interface (Fig. 1d). Specimens with remaining enamel or premature debonding were excluded from the MTBS test. Each molar produced one beam. A total of 20 beams were tested in each group (n=20).

MTBS test

The prepared beams were fixed to the testing jig using cyanoacrylate glue (Zapit, Dental Venture of America, Corona, CA, USA), and subjected to the MTBS test in a universal testing machine (EZ-SX 500N, Shimadzu, Kyoto, Japan). The specimens were tested with a crosshead speed of 1 mm/min, and the bond strength values (MPa) were measured (Fig. 1e).

Fractography with OCT

Prior to MTBS testing, each beam was assessed using SS-OCT to observe the interface between the dentin and resin. The specimens were positioned horizontally on the head stage, and the scanning beam was applied perpendicular to the lateral sides of the specimens. B-scans of each section were recorded at 250 μm intervals for 3 images totally to observe the interface between dentin and resin (Fig. 1d). After the MTBS test, the debonded specimens were observed using SS-OCT to visualize internal crack formation within the dentin. Specimens were positioned perpendicular on the head stage and the scanning beam was projected perpendicular to the debonded interface to obtain cross-sectional images at 250 μm intervals. The specimens were then rotated in 90° increments to get another images at 250 μm intervals. As a result, 6 images of 250 μm intervals totally were recorded from each debonded interface (Fig. 1f). Next, 2-D cross-sectional images were imported into image analysis software (ImageJ version 42.1q, National Institutes of Health, Bethesda, MD, USA). Based on the binarization process[24], a software plugin was used to recognize the target pixels with higher brightness compared to the surrounding pixels. These appeared as a white spots and lines and indicated cracks at bonding interfaces. At each cross section, a region of interest (ROI) was selected as a rectangle below the interface with the width equal to the specimen width and a height of 500 μm (optical) covering the white clusters (Fig. 2a). The distribution percentage of these pixels over the ROI area was measured automatically by the plugin to calculate subsurface cracks at each cross section (Fig. 2b).

Fracture mode

Interfaces that were debonded after the MTBS test were assessed using confocal laser scanning microscope (CLSM; VK-X150, Keyence, Osaka, Japan) and scanning electronic microscopy (SEM; JSM-IT100, JEOL, Tokyo, Japan) to determine the mode of failure (Fig. 1g). The failure mode of each beam was classified into five categories: A, >95% cohesive failure in dentin; B, >50%

failure in dentin; C, adhesive failure, D; >50% failure in resin; E, >95% cohesive failure in resin.

Confirmation of SS-OCT findings

Representative debonded specimens were embedded into epoxy resin (Buehler) to confirm the presence or absence of an internal dentin crack. Lateral sides of the specimens were polished to reach the middle section of the beam using a polishing machine (ML-160A, Maruto, Tokyo, Japan) with 1500 and 2000 grit SiC papers, followed by diamond pastes with a particle size down to 1 μm under running water. The corresponding interfacial location as the cross-sectional OCT image was observed using CLSM and SEM.

Statistical analysis

The MTBS and crack formation data were analyzed using Kruskal Wallis and Mann Whitney's *U* tests with the Bonferroni's correction. Modes of failure for each group were analyzed using the chi-square test. All statistical procedures were performed at a significant level of α=0.05 with Statistical Package for the Social Sciences (SPSS ver.16.0 for windows, IBM, Chicago, IL, USA).

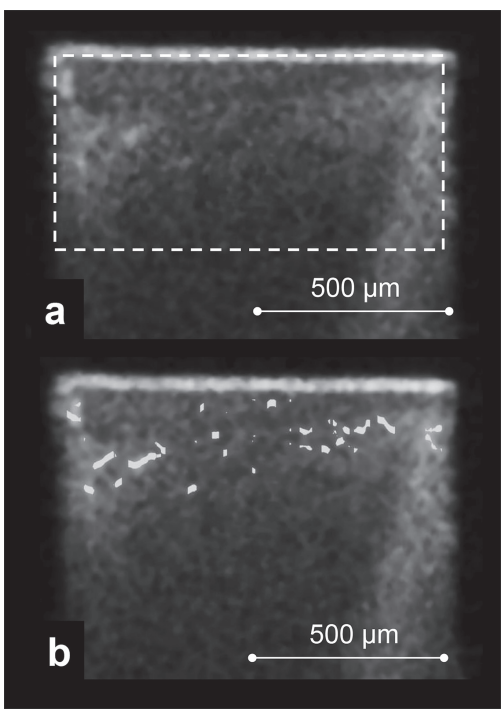

Fig. 2 (a) Cross sectional SS-OCT image of dentin part of debonded specimen. The region of interest was selected to be analyzed using ImageJ (version 1.42q) on 2D-scan images. Selected region of interest was appeared as the area surrounded by dot lines, designating the presence of internal fracture in dentin. The brighter pixels indicate significantly higher intensity signals at the interfacial zone. (b) Post-algorithm image.

RESULTS

A representative SS-OCT image of the samples before and after MTBS test is shown in Fig. 3. After MTBS test, numerous globular zones or dots with increased brightness were observed at the debonded subsurface zone, suggesting the presence of internal damage. Mean MTBS in each group is shown in Fig. 4. Deep dentin had lower MTBS than superficial dentin (Kruskal Wallies, p<0.05), especially without lining (Mann Whitney U, p<0.05). The use of lining increased the MTBS in deep dentin, but this did not reach significance (p>0.05).

There was a significant difference in the formation of internal dentin fracture between location (superficial and deep) and placement technique (with and without flowable liner, p<0.05; Fig. 5). Deep dentin showed an increased bright zone area when compared with superficial dentin (p<0.05). Moreover, the use of flowable lining significantly decreased the formation of internal fracture (p<0.05).

A representative CLSM and SEM images of five classifications in failure mode of the samples after MTBS test are shown in Fig. 6. Chi-square tests revealed that there was a significant difference in the frequency of fracture pattern between placement technique (with and without flowable liner, p<0.05). No significant difference was observed between dentin locations (p>0.05; Fig. 7 and Table 2).

SS-OCT imaging after MTBS test revealed internal

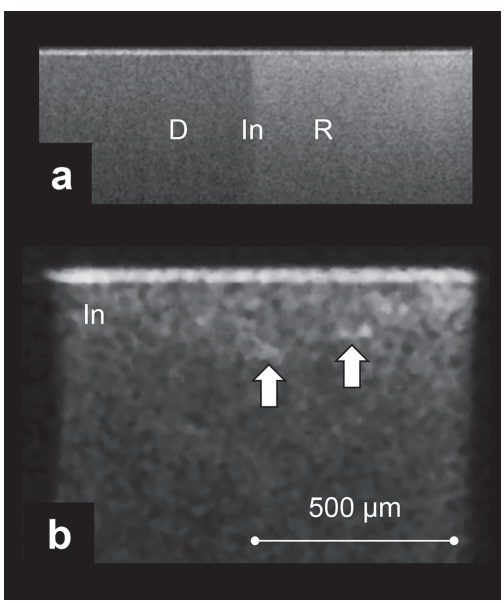

Fig. 3 SS-OCT images obtained from the MTBS test beams.
(a) Specimens with no crack at the interface observed before MTBS test. (b) The dentin part of debonded specimen with fracture appeared as bright dots and lines below the interface. MTBS, microtensile bond strength; R, resin composite; D, dentin; In, interface; arrow, fracture formation.

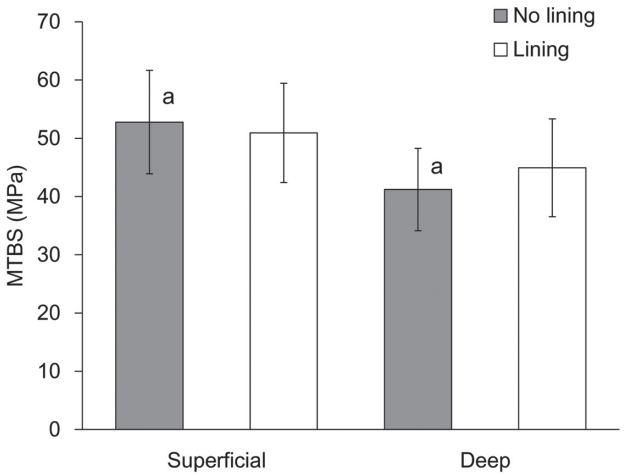

Fig. 4 Charts presenting the MTBS of each group.
Same lowercase letter indicates significant difference between the groups (p<0.05).

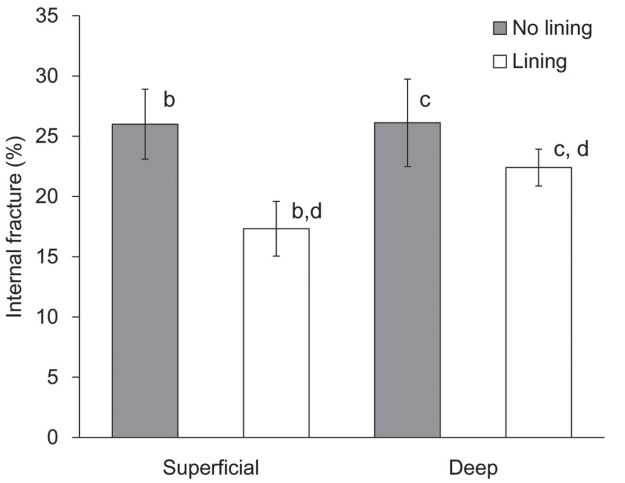

Fig. 5 Charts presenting the percentage of internal dentin fracture in each group.
Application of flowable lining significantly reduced dentin fracture in both locations. Same lowercase letter indicates significant difference between the groups (p<0.05).

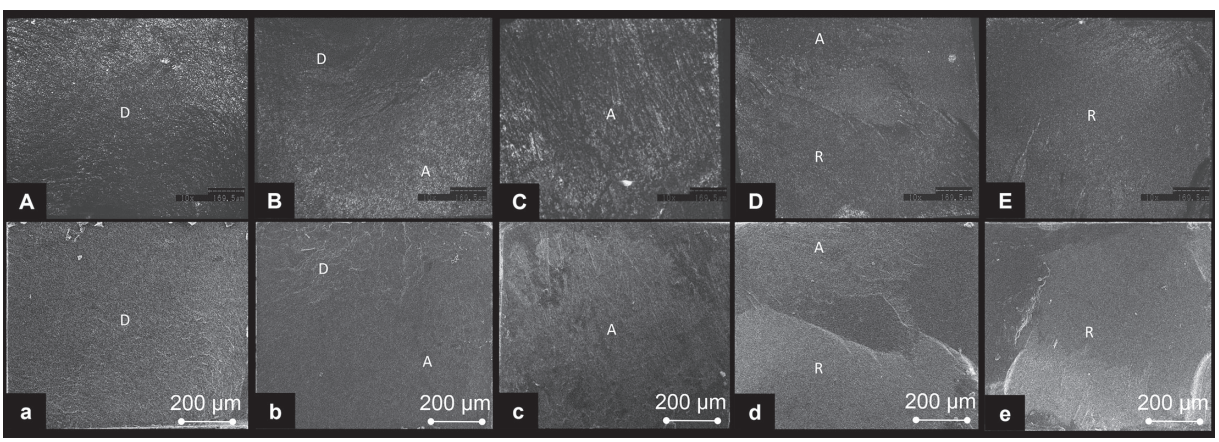

Fig. 6 CLSM (A–E) and SEM (a–e) images of five categorizations in failure mode.
(A, a) >95% cohesive failure in dentin, (B, b) >50% cohesive failure in dentin, (C, c) adhesive failure, (D, d) >50% failure in resin, (E, e) >95% cohesive failure in resin. D, dentin; A, adhesive; R, resin composite.

fracture at the dentin side of debonded specimens (Fig. 8a). The fracture patterns on the image appeared as dots and lines roughly parallel to the interface, with increased signal intensity (Fig. 8b). These findings were confirmed using cross-sectional CLSM (Fig. 8c) and SEM images (Fig. 8d) at the same location. Some of the samples after MTBS test showed the presence of resin remained on the debonded interface suggesting the fracture of resin (Fig. 9).

DISCUSSION

OCT is an interferometry technique that can provide cross sectional images of internal biological tissues with

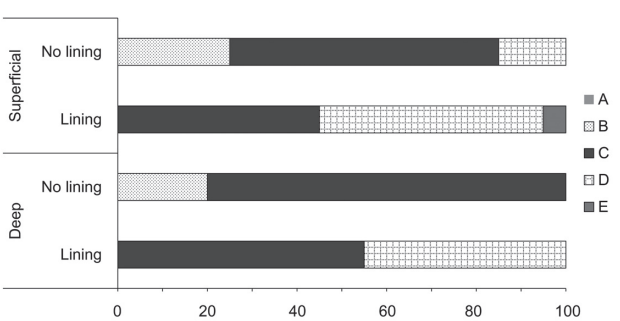

Fig. 7 Summary of failure mode for the test groups.

Table 2 Failure mode analysis using the chi-square test

	No lining					Lining					
	A	B	C	D	E	A	B	C	D	E	
Superficial	0	5	12	3	0	0	0	9	10	1	$p<0.05$ $\chi^2=5.70078$
Deep	0	4	16	0	0	0	0	11	9	0	$p<0.05$ $\chi^2=10.9298$
			$p>0.05$ $\chi^2=1.98737$					$p>0.05$ $\chi^2=0.385720$			

A, >95% cohesive failure in dentin; B, >50% failure in dentin;
C, adhesive failure; D, >50% failure in resin; E, >95% cohesive failure in resin

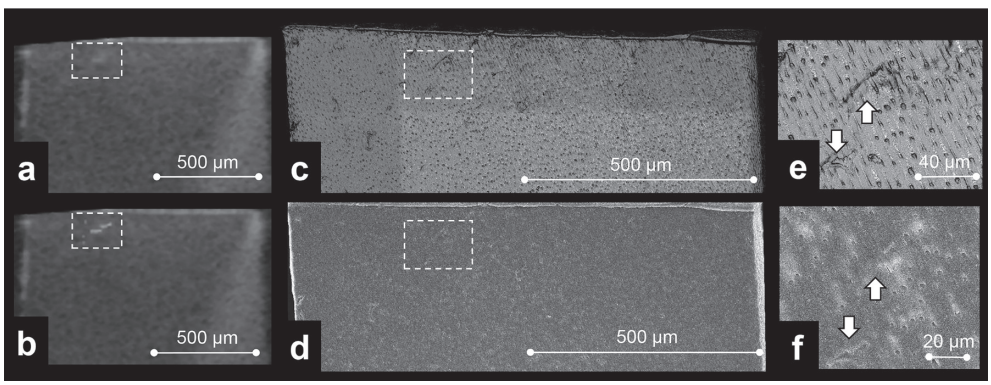

Fig. 8 (a) Representative cross-sectional SS-OCT image of the dentin side of the specimen after the MTBS test. Internal dentin fracture occurred at the location surrounded by dot lined square. (b) Post-algorithm image analyzed by ImageJ. (c) Cross-sectional CLSM image of (a) at the same observation location. Dot lined square in (c) indicates the corresponding dotted square in (a) and (b). (d) SEM image of (c). (e) CLSM image at higher magnification of (c). Presence of internal dentin fracture was observed (arrows). (f) Corresponding SEM image of (e). Internal dentin fracture (arrows).

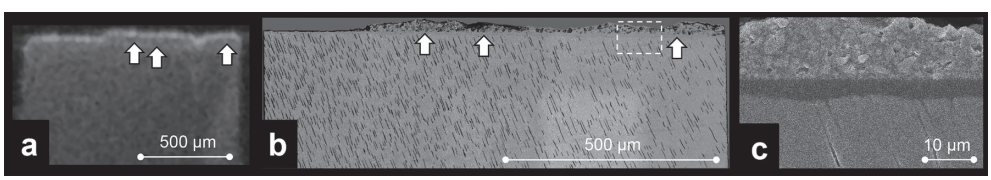

Fig. 9 (a) Representative SS-OCT image of MTBS test sample with composite resin fracture. Despite the image was not clear due to the limitation of space resolving power, SS-OCT could image the presence of resin remained on the debonded surface (arrows). (b) CLSM image at same cross section as (a). Remnant of resin was clearly visualized (arrows). (c) SEM image of area of dot line in (b).

real-time acquisition. OCT has been used to demarcate the presence of diseases with high spatial resolution based on variations in the optical properties within the structure[26]. This modality has been used in dentistry to detect gap formation differences between resin-based restoration and dental tissue[8,23,24], and enamel and dentin cracks[10,25,26]. SS-OCT is one of the latest versions of OCT that employs the laser light sweeping wavelength to construct cross-sectional image with improved penetration depth. Recently, SS-OCT was employed to evaluate the fracture mode after the tensile bond test and shear bond test to detect the internal fracture within the substrate[10,27]. It has been shown that increased signal brightness in gray scale OCT images corresponds to the defect location[10,23].

In this study, SS-OCT was used to monitor the

internal structure of dentin after MTBS testing. As a result, dentin fractures below the interface were observed as bright pixels. The size of the bright zone after MTBS testing was significantly influenced by dentin locations and placement technique. Deep dentin caused a larger internal fracture than superficial dentin, whereas flowable lining reduced the formation of an internal fracture. The region of exhibiting bright pixels in SS-OCT image corresponded to the location of the internal fracture in dentin observed *via* CLSM and SEM (Fig. 8c, d), which confirmed the location of fracture in dentin.

In accordance with previous studies, superficial dentin showed higher MTBS than deep dentin, and this effect was more prominent in samples without flowable lining[28-33]. The usage of flowable lining could decrease the difference of MTBS for the two locations as a result of increased bond strength of deep dentin. Moreover, SS-OCT analysis clearly showed a protective effect of flowable lining for deep dentin; however, the area of crack formation was more evident in deep dentin than superficial dentin.

The CLSM images that assessed the failure mode after MTBS testing showed that adhesive failure was most predominant for samples without flowable lining. This indicates that the usage of lining could remarkably reduce the occurrence of dentin fracture; however, it may increase the cohesive failure of resin within the fracture surface. In this study, some of the samples after MEBS test showed the presence of resin remained on the debonded surface suggesting the partial fracture of resin (Fig. 9). Despite the image was not clear due to the limitation of special resolution, SS-OCT could also visualize the remnant of resin remained on the debonded surface.

The use of restorative materials and dentin with different elastic moduli creates an elastic mismatch that may change the stress distribution and degrees of deformation in direct dental restoration[34]. In this study, we used Clearfil Majesty ES Flow for the material for lining. This material is classified as a nanohybrid flowable resin containing 59% filler, with 0.18–3.5 μm particle[35]. Its elastic modulus is 6.6 GPa, which is markedly lower than Clearfil AP-X (16.8 GPa). The elastic modulus of dentin is influenced by its depth; superficial and deep dentin exhibit elastic moduli of 15 and 13 GPa, respectively[36]. Consequently, the elastic mismatch between flowable lining and dentin or hybrid resin is greater than the difference between dentin and composite resin in the samples without lining, and this may influence the stress distribution within the sample to move the fracture area.

Cracks form when the maximum tensile stress exceeds the elastic limit of the material[34,37], resulting in the crack initiation and deformation at weakest point of interface. Meanwhile cohesive failure is explained by the mechanics of the test and the brittleness of the materials involved[38]; the cohesive failure of resin for lining is associated with local stress that exceeds the elastic limit of the lining. Therefore, the reduction in dentin fractures with the use of lining may be due to the elastic limit of the flowable lining conferring a protective effect for the underlining dentin during MTBS testing.

Depth-associated variations in dentin components include tubule density and diameter. In addition, the mineral contents of the matrix influence mechanical properties, such as elastic modulus, which reduces the position moves from the DEJ to the pulp[18,36,39]. In this study, the reduced mechanical properties of deep dentin induced a lower resistance to fracture, which resulted in lower bond strength and increased internal fracture formation when compared with superficial dentin.

Interfacial integrity is critical for the longevity of adhesive restorations. The results of this study suggest that dentin could be deteriorated through internal fracture formation because of different modes of stress concentration at the interface. Although the mode of stress applied in this study was tensile, stress distribution within the substrate is not homogeneous mixed with tensile and shear[38]. Consequently, presence of dentin fracture blow the interface appears to show the heterogeneous stress distribution occurred along the interface during the test. Despite further study is necessary to clarify the clinical significance of internal dentin fracture formation after the MTBS test, less internal damage appears advantageous for the longevity of restorations in clinical situation under occlusal function.

The null hypothesis of this study was rejected: the use of flowable lining significantly influenced the formation of internal dentin fracture and reduced the differences in MTBS between dentin locations. This suggests that the use of flowable lining for direct composite restorations could increase bond strength to deep dentin and prevent of internal dentin fracture in MTBS testing. Consequently, the use of flowable lining in deep cavities appears advantageous for direct composite restorations to achieve excellent prognosis and improved longevity. Further studies will be necessary to investigate the effect of flowable lining on other clinical factors that influence the adhesive restorations and internal fracture formation.

CONCLUSION

Within the limitation of this study, the usage of flowable lining behaved to prevent internal dentin fracture with increasing MTBS. Furthermore, the influence of dentin depth on MTBS was reduced with the usage of flowable lining. Finally, we have demonstrated that SS-OCT imaging has an effective detecting of cracks in the substrate. Further studies analyzing internal dentin fracture under loading must be necessary.

ACKNOWLEDGMENTS

This work was supported by Research Grant for Longevity Science (29-3) from Ministry of Health, Labor and Welfare, Japan and by Grant-in-Aid for Scientific Research (16K11544) from Japan Society for the Promotion of Science (JSPS).

REFERENCES

1) Swift EJ, Triolo PT, Barkmeier WW, Bird JL, Bounds SJ. Effect of low-viscosity resins on the performance of dental adhesives. Am J Dent 1996; 9: 100-104.
2) Van Meerbeek B, Willems G, Celis JP, Roos JR, Braem M, Lambrechts P, *et al.* Assessment by nano-indentation of the hardness and elasticity of the resin-dentin bonding area. J Dent Res 1993; 72: 1434-1442.
3) Kemp-Scholte CM, Davidson C. Complete marginal seal of class V resin composite restorations effected by increased flexibility. J Dent Res 1990; 69: 1240-1243.
4) De Goes MF, Giannini M, di Hipólito V, Carrilho MR de O, Daronch M, Rueggeberg FA. Microtensile bond strength of adhesive systems to dentin with or without application of an intermediate flowable resin layer. Braz Dent J 2008; 19: 51-56.
5) Giannini M, De Goes MF, Nikaido T, Shimada Y, Tagami J. Influence of activation mode of dual-cured resin composite cores and low-viscosity composite liners on bond strength to dentin treated with self-etching adhesives. J Adhes Dent 2004; 6: 301-306.
6) Shahidi C, Krejci I, Dietschi D. In vitro evaluation of marginal adaptation of direct class II composite restorations made of different "low-shrinkage" systems. Oper Dent 2017; 42: 273-283.
7) Haak R, Wicht MJ, Noack MJ. Marginal and internal adaptation of extended class I restorations lined with flowable composites. J Dent 2003; 31: 231-239.
8) Yoshimine N, Shimada Y, Tagami J, Sadr A. Interfacial adaptation of composite restorations before and after light curing: Effects of adhesive and filling technique. J Adhes Dent 2015; 17: 329-336.
9) Anatavara S, Sitthiseripratip K, Senawongse P. Stress relieving behaviour of flowable composite liners: A finite element analysis. Dent Mater J 2016; 35: 369-378.
10) Dao Luong MN, Shimada Y, Turkistani A, Tagami J, Sumi Y, Sadr A. Fractography of interface after microtensile bond strength test using swept-source optical coherence tomography. Dent Mater 2016; 32: 862-869.
11) Van Meerbeek B, De Munck J, Yoshida Y, Inoue S, Vargas M, Vijay P, *et al.* Adhesion to enamel and dentin: Current status and future challenges. Oper Dent 2003; 28: 215-235.
12) Sarr M, Kane AW, Vreven J, Mine A, Van Landuyt KL, Peumans M, *et al.* Microtensile bond strength and interfacial characterization of 11 contemporary adhesives bonded to bur-cut dentin. Oper Dent 2010; 35: 94-104.
13) Yoshida Y, Nagakane K, Fukuda R, Nakayama Y, Okazaki M, Shintani H, *et al.* Comparative study on adhesive performance of functional monomers. J Dent Res 2004; 83: 454-458.
14) Sano H, Shono T, Sonoda H, Takatsu T, Ciucchi B, Carvalho R, *et al.* Relationship between surface area for adhesion and tensile bond strength - Evaluation of a micro-tensile bond test. Dent Mater 1994; 10: 236-240.
15) Sano H, Yoshikawa T, Pereira RNR, Kanemura N, Morigami M, Tagami J, *et al.* Long-term durability of dentin bonds made with a self-etching primer, in vivo. J Dent Res 1999; 78: 906-911.
16) Giannini M, Carvalho RM, Martins LR, Dias CT, Pashley DH. The influence of tubule density and area of solid dentin on bond strength of two adhesive systems to dentin. J Adhes Dent 2001; 3: 315-324.
17) De Goes MF, Giannini M, Foxton R, Nikaido T, Tagami J. Microtensile bond strength between crown and root dentin and two adhesive systems. J Prosthet Dent 2007; 97: 223-228.
18) Marshall GW, Marshall SJ, Kinney JH, Balooch M. The dentin substrate: Structure and properties related to bonding. J Dent 1997; 25: 441-458.
19) Pashley DH, Okabe A, Parham P. The relationship between dentin microhardness and tubule density. Endod Dent Traumatol 1985; 1: 176-179.
20) Shimada Y, Sadr A, Sumi Y, Tagami J. Application of optical coherence tomography (OCT) for diagnosis of caries, cracks, and defects of restorations. Curr Oral Heal Reports 2015; 2: 73-80.
21) Shimada Y, Sadr A, Burrow MF, Tagami J, Ozawa N, Sumi Y. Validation of swept-source optical coherence tomography (SS-OCT) for the diagnosis of occlusal caries. J Dent 2010; 38: 655-665.
22) Nakagawa H, Sadr A, Shimada Y, Tagami J, Sumi Y. Validation of swept source optical coherence tomography (SS-OCT) for the diagnosis of smooth surface caries in vitro. J Dent 2013; 41: 80-89.
23) Bakhsh TA, Sadr A, Shimada Y, Tagami J, Sumi Y. Non-invasive quantification of resin-dentin interfacial gaps using optical coherence tomography: Validation against confocal microscopy. Dent Mater 2011; 27: 915-925.
24) Sadr A, Shimada Y, Mayoral JR, Hariri I, Bakhsh TA, Sumi Y, *et al.* Swept source optical coherence tomography for quantitative and qualitative assessment of dental composite restorations. Proc SPIE 2011; 7884: 78840C-1.
25) Nakajima Y, Shimada Y, Miyashin M, Takagi Y, Tagami J, Sumi Y. Noninvasive cross-sectional imaging of incomplete crown fractures (cracks) using swept-source optical coherence tomography. Int Endod J 2012; 45: 933-941.
26) Imai K, Shimada Y, Sadr A, Sumi Y, Tagami J. Noninvasive cross-sectional visualization of enamel cracks by optical coherence tomography in vitro. J Endod 2012; 38: 1269-1274.
27) Makishi P, Pacheco RR, Sadr A, Shimada Y, Sumi Y, Tagami J, *et al.* Assessment of self-adhesive resin composites: Nondestructive imaging of resin - dentin interfacial adaptation and shear bond strength. Microsc Microanal 2015; 21: 1523-1529.
28) Watanabe LG, Marshall GW, Marshall SJ. Dentin shear strength: effects of tubule orientation and intratooth location. Dent Mater 1996; 12: 109-115.
29) Konishi N, Watanabe LG, Hilton JF, Marshall GW, Marshall SJ, Staninec M. Dentin shear strength: Effect of distance from the pulp. Dent Mater 2002; 18: 516-520.
30) Inoue S, Pereira PNR, Kawamoto C, Nakajima M, Koshiro K, Tagami J, *et al.* Effect of depth and tubule direction on ultimate tensile strength of human coronal dentin. Dent Mater J 2003; 22: 39-47.
31) Inoue T, Takahashi H, Nishimura F. Anisotropy of tensile strengths of bovine dentin regarding dentinal tubule orientation and location. Dent Mater J 2002; 21: 32-43.
32) Villela-Rosa ACM, Gonçalves M, Orsi IA, Miani PK. Shear bond strength of self-etch and total-etch bonding systems at different dentin depths. Braz Oral Res 2011; 25: 109-115.
33) Burrow MF, Takakura H, Nakajima M, Inai N, Tagami J, Takatsu T. The influence of age and depth of dentin on bonding. Dent Mater 1994; 10: 241-246.
34) Yao H, Xie Z, He C, Dao M. Fracture mode control: a bio-inspired strategy to combat catastrophic damage. Sci Rep 2015; 5: 1-6.
35) Randolph LD, Palin WM, Leloup G, Leprince JG. Filler characteristics of modern dental resin composites and their influence on physico-mechanical properties. Dent Mater 2016; 32: 1586-1599.
36) Ryou H, Amin N, Ross A, Eidelman N, Wang DH, Romberg E, *et al.* Contributions of microstructure and chemical composition to the mechanical properties of dentin. J Mater Sci Mater Med 2011; 22: 1127-1135.
37) Rankine WJM. On the stability of loose earth. Phil Trans R Soc Lond 1857; 147: 9-27.
38) Braga RR, Meira JBC, Boaro LCC, Xavier TA. Adhesion to tooth structure: A critical review of "macro" test methods. Dent Mater 2010; 26: e38-49.
39) Marshall GW. Dentin: microstructure and characterization. Quintessence Int 1993; 24: 606-617.